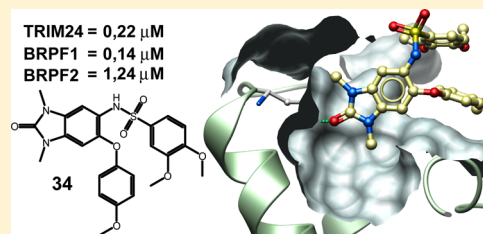


## Discovery of a Chemical Tool Inhibitor Targeting the Bromodomains of TRIM24 and BRPF

James Bennett,<sup>†,‡</sup> Oleg Fedorov,<sup>†,‡</sup> Cynthia Tallant,<sup>†,‡</sup> Octovia Monteiro,<sup>†,‡</sup> Julia Meier,<sup>‡</sup> Vicky Gamble,<sup>‡</sup> Pavel Savitsky,<sup>†,‡</sup> Graciela A Nunez-Alonso,<sup>†,‡</sup> Bernard Haendler,<sup>||</sup> Catherine Rogers,<sup>†,‡</sup> Paul E. Brennan,<sup>†,‡</sup> Susanne Müller,<sup>†,‡</sup> and Stefan Knapp<sup>\*,†,‡,§</sup><sup>†</sup>The Structural Genomic Consortium, University of Oxford, Old Road Campus Research Building, Roosevelt Drive, Headington, Oxford OX3 7DQ, U.K.<sup>‡</sup>Target Discovery Institute, University of Oxford, NDM Research Building, Roosevelt Drive, Headington, Oxford OX3 7FZ, U.K.<sup>§</sup>Institute for Pharmaceutical Chemistry, Johann Wolfgang Goethe-University, Max-von-Laue-Strasse 9 D-60438 Frankfurt am Main, Germany<sup>||</sup>Global Drug Discovery, Bayer Pharma AG, Müllerstrasse 178, D-13353 Berlin, Germany

## S Supporting Information

**ABSTRACT:** TRIM24 is a transcriptional regulator as well as an E3 ubiquitin ligase. It is overexpressed in diverse tumors, and high expression levels have been linked to poor prognosis in breast cancer patients. TRIM24 contains a PHD/bromodomain offering the opportunity to develop protein interaction inhibitors that target this protein interaction module. Here we identified potent acetyl-lysine mimetic benzimidazolones TRIM24 bromodomain inhibitors. The best compound of this series is a selective BRPF1B/TRIM24 dual inhibitor that bound with a  $K_D$  of 137 and 222 nM, respectively, but exerted good selectivity over other bromodomains. Cellular activity of the inhibitor was demonstrated using FRAP assays as well as cell viability data.



## INTRODUCTION

Bromodomains are acetyl-lysine specific epigenetic effector domains that have emerged as new targets for the design of protein interaction inhibitors modulating gene transcription and chromatin structure.<sup>1,2</sup> Targeting bromodomains received a lot of attention recently after selective inhibitors of BET (bromo and extra-terminal) bromodomains showed excellent efficacy in a number of cancer models<sup>3–7</sup> as well as in inflammation<sup>8</sup> and first inhibitors entered now in clinical testing. Since then, targeting bromodomains has been mainly focused on BET family members with only few tool compounds available for non-BET bromodomains.<sup>9–12</sup> However, favorable druggability has been predicted for many bromodomains<sup>13</sup> and the family is well covered in terms of available crystal structures enabling rational design of selective tool compounds.<sup>14,15</sup> The excellent druggability of bromodomains has recently been demonstrated by high hit rates<sup>16</sup> as well as the frequent potent activity of inhibitors developed for other targets such as kinases.<sup>17,18</sup>

Tripartite motif 24 protein (TRIM24), also known as TIF1 $\alpha$ , contains a plant homeodomain/bromodomain dual epigenetic reader domain and a RING type E3 ubiquitin ligase domain. TRIM24 overexpression has been recently associated with poor overall survival and tumor progression of breast-cancer patients,<sup>19</sup> and high expression levels have been reported in glioblastoma,<sup>20</sup> hepatocellular carcinoma,<sup>21</sup> gastric cancer,<sup>22</sup> non-small cell lung cancer,<sup>23</sup> and head and neck squamous cell

carcinoma.<sup>24</sup> In addition, in prostate cancer, TRIM24 is upregulated by mutations in SPOP, an E3 ubiquitin ligase substrate-binding protein.<sup>25</sup> TRIM24 acts as an E3-ubiquitin ligase of p53, promoting degradation of this key DNA damage regulator.<sup>26</sup> Furthermore, it functions as a coactivator of the estrogen receptor<sup>19</sup> and it interacts with the ligand bound retinoic acid (RA) receptor repressing its transcriptional activity.<sup>27</sup> Knockdown of TRIM24 in lung cancer cells decreased the protein levels of a number of cyclins and p-Rb and increased p27 expression,<sup>23</sup> whereas a recent knockdown study of TRIM24 in colon cancer cell lines showed that deletion of this protein impairs cell growth and leads to induction of apoptosis.<sup>28</sup> Thus, TRIM24 may regulate levels of cancer-relevant proteins on the transcriptional as well as the protein level.

A recent study showed that ectopic expression of TRIM24 in isogenic human mammary epithelial cells (HMEC) increased cellular proliferation and induced malignant transformation. Transcription analysis of these cells revealed a glycolytic and tricarboxylic acid cycle gene signature, resulting in increased glucose uptake and activated aerobic glycolysis.<sup>29</sup> However, a tumor suppressor function of TRIM24 has also been suggested.

Special Issue: Epigenetics

Received: March 20, 2015

Published: May 14, 2015

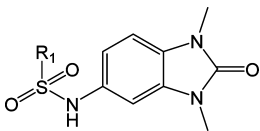
Deletion of TRIM24 in mice results in cell cycle defects, leading to the development of liver cancer as a result of retinoic acid receptor repression.<sup>30</sup>

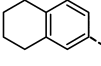
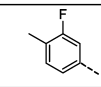
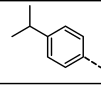
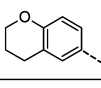
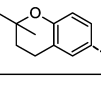
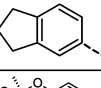
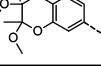
The three-dimensional structure of the TRIM24 PHD/bromodomain revealed that this dual reader domain functions as a cooperative unit recognizing unmodified H3K4 with its PHD zinc finger domain and H3K23ac with its bromodomain.<sup>19</sup> The context dependent and complex roles of TRIM24 in regulating protein turnover and transcription and its role in cancer raise the question of the consequences of inhibition of druggable domains in TRIM24 such as the bromodomain. To enable functional studies addressing this issue and the potential of targeting the TRIM24 bromodomain for cancer therapy, we developed a potent chemical tool molecule based on the 1,3 benzimidazolone scaffold, which has been recently identified as an acetyl-lysine competitive inhibitor of bromodomains of the BRPF family.<sup>11</sup>

## RESULTS AND DISCUSSION

To develop a TRIM24 specific inhibitor, we used an Alpha Screen assay to evaluate commercial 1,3 benzimidazolones that were all decorated with a sulfonamide substitution in position 5 and had a number of different substituents in R1. These inhibitors had nM IC<sub>50</sub> values for BRPF1B and about 10-fold less potency for the closely related BRPF2 (BRD1). However, the most interesting compounds of this series (3–5) also had 3–4 μM activity against TRIM24, which prompted us to explore this scaffold for the development of TRIM24 inhibitors (Table 1).

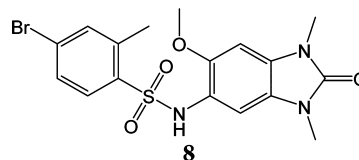
**Table 1. Influence of R1 Substituted Benzimidazolones on BRPF1, BRPF2, and TRIM24 Bromodomain Activity<sup>a</sup>**



Comp	R1	TRIM24 IC <sub>50</sub> (μM)	BRPF1 IC <sub>50</sub> (μM)	BRPF2 IC <sub>50</sub> (μM)
1		6.17 ± 0.72	0.33 ± 0.08	2.05 ± 0.93
2		>10	0.59 ± 0.05	6.14 ± 0.27
3		3.45 ± 0.14	0.42 ± 0.002	4.3 ± 0.22
4		4.63 ± 4.11	0.27 ± 0.09	1.60 ± 0.68
5		3.69 ± 1.49	0.31 ± 0.11	2.46 ± 0.98
6		>10	0.29 ± 0.07	1.71 ± 0.55
7		>10	1.4 ± 0.002	>10

<sup>a</sup>Shown are averaged values of three measurements as well as SEM.

Next we explored substitution in position 6. The methoxy analogue **8** lost activity against TRIM24 but was still a potent BRPF bromodomain inhibitor (IC<sub>50</sub> values of 0.27 and 1.2 μM, respectively).



This trend was observed for all compounds that harbored a methoxy group in R2 and variations in R1 (compounds 9–22 Supporting Information Table 1). The R2 methoxy group resulted also in inactivity for BRD4(1). However, phenoxy substitutions in position 6 considerably improved TRIM24 activity (Table 2).

In particular, compound **24** showed IC<sub>50</sub> values of 480 nM for the bromodomain of TRIM24. However, inhibitors of this series were still more potent for BRPF1B and BRPF2 bromodomains.

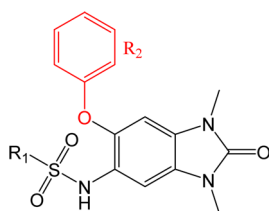
We explored therefore different substitutions in position 6 in combination with R1 (Supporting Information Table 1). Interestingly, methoxy-phenoxy substituted inhibitors showed good activity for TRIM24 but selectivity over BRPF bromodomains was not achieved (Table 3). The best inhibitor of this series has an IC<sub>50</sub> value of 0.43 μM for TRIM24 and 0.34 μM for BRPF1, respectively.

We characterized the TRIM24/BRPF dual bromodomain inhibitor further. Isothermal titration calorimetry data showed that **34** bound the TRIM24 bromodomain with a *K<sub>D</sub>* of 222 nM (Figure 1) and had a *K<sub>D</sub>* for the BRPF1 bromodomain of 137 nM and for BRD1 of 1130 nM. Binding to BRPF3 was considerably weaker, resulting in an AlphaScreen IC<sub>50</sub> value of about 7 μM. Binding was strongly driven by enthalpy, with a large favorable enthalpy change of −12.1, −15.7, and −12.1 kcal/mol for TRIM24, BRPF1 and BRD1, respectively, and was opposed by entropy (*TΔS* of −3.2 kcal/mol (TRIM24) and −6.5 kcal/mol (BRPF1)). A table of all fitted parameters and a figure of titration data has been included in Supporting Information Figure 1.

Next we evaluated the selectivity of **34** against a comprehensive panel of bromodomains using a temperature shift assay.<sup>31</sup> By screening a panel of 45 bromodomains, we found excellent selectivity of **34** for BRPF1B/2 and TRIM24 (Figure 2).

To get insight into the binding mode of **34**, we determined the cocrystal structure with the TRIM24 PHD/bromodomain.

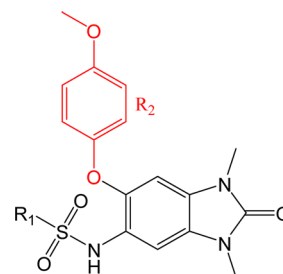
The TRIM24 cocrystal structure revealed the expected globular domain organization of the PHD and bromodomain, showing tight interaction between the two reader domains (Figure 3a).<sup>19</sup> The inhibitor was well-defined by electron density, and **34** showed the expected binding mode of the acetyl-lysine mimetic benzimidazolones moiety (Figure 3b),<sup>11</sup> forming the canonical hydrogen bond with the conserved asparagine N980 and a water mediated hydrogen bond to Y935 linking the inhibitor also to the conserved water network at the bottom of the binding pocket. Interestingly, the two aromatic rings stack against the ZA loop, effectively occupying the space at the rim of the acetyl-lysine binding site, a binding mode that has recently been reported also for a BAZ2B bromodomain inhibitor.<sup>32</sup> Similar to the stacking conformation observed in BAZ2B, it is likely that this inhibitor conformation is not the

Table 2. 6-Phenoxy Substituted Inhibitors with Variations in R1<sup>a</sup>

Comp	R1	TRIM24 IC50 (μM)	BRPF1 IC50 (μM)	BRPF2 IC50 (μM)
23		1.56 ± 0.29	0.27 ± 0.09	3.47 ± 0.1
24		0.48 ± 0.13	0.29 ± 0.003	1.21 ± 0.03
25		4.77 ± 2.51	3.10 ± 2.40	5.16 ± 0.06
26		0.74 ± 0.21	0.34 ± 0.05	1.33 ± 0.31
27		2.45 ± 0.50	1.17 ± 0.01	2.39 ± 0.19
28		2.70 ± 0.56	1.05 ± 0.014	3.69 ± 0.38
29		3.42 ± 0.90	0.79 ± 0.005	2.42 ± 0.05
30		1.27 ± 0.10	0.51 ± 0.008	2.92 ± nd
31		2.62 ± 0.20	0.43 ± 0.12	1.70 ± 0.04
32		2.38 ± 0.18	0.43 ± 0.12	1.99 ± 0.14
33		>10	2.68 ± 0.73	2.67 ± nd

<sup>a</sup>Shown are averaged values of three measurements as well as SEM.

prevalent conformation in solution, providing potentially a rationale for the observed unfavorable binding entropy measured in the ITC experiments. The R2 methoxy phenyl ring fits perfectly into a hydrophobic cavity lined by A923 and L922, explaining the loss of binding activity for R2 methoxy substitutions. The benzimidazolone ring forms mainly hydrophobic interactions with residues on both sites of the acetyl-lysine binding cavity (V932, V928, V986, P929). SAR revealed that the sulfonamide substitutions (R1) can tolerate many different ring systems. This observation is compatible with the crystal structure, which shows that this substituent is in a solvent exposed position. However, polar interactions of the R1 aromatic decoration with residues in the BC loop (E985) could

Table 3. 6-*para*-Methoxy-phenoxy Substituted Inhibitors with Variations in R1<sup>a</sup>

Co mp	R1	TRIM24 IC50 (μM)	BRPF1 IC50 (μM)	BRPF2 IC50 (μM)
34		0.43 ± 0.20	0.34 ± 0.08	1.75 ± 0.45
35		0.73 ± 0.18	0.66 ± 0.01	2.77 ± 0.24
36		0.77 ± 0.26	0.66 ± 0.002	3.58 ± 0.09
37		1.47 ± 0.26	0.68 ± 0.01	2.38 ± 0.003
38		8.40 ± nd	6.72 ± 0.084	>10
39		2.70 ± 0.53	2.24 ± 0.039	>10

<sup>a</sup>Shown are averaged values of three measurements as well as SEM.

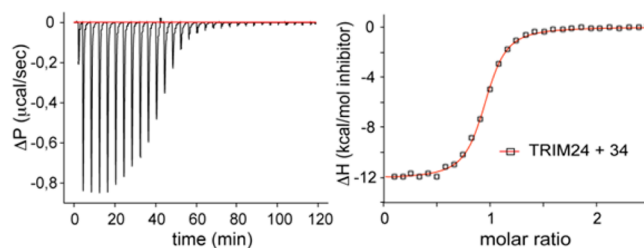


**Figure 1.** ITC data measured using **34** and the PHD/bromodomain of TRIM24. Shown are raw heat effects (left panel) of 30 consecutive injections of TRIM24 injected in a solution of **34** in 20 mM HEPES buffer, pH 7.5, 150 mM NaCl, and 0.5 mM TCEP. Normalized injection heats as well as a nonlinear least-squares fit for a single binding site model are shown in the right panel.

potentially increase potency and specificity for TRIM24 as BRPF1B has an isoleucine at this position. Crystallographic data collection statistics are summarized in Supporting Information Table 2, and additional figures including a comparison with acetyl-lysine containing peptide complexes have been included in Supporting Information Figure 2. Comparison of the BRPF1B and BRD1 (BRPF2) acetyl-lysine binding site are shown in Figure 3c as well as in Supporting Information Figure 2. As expected, residues contacting **34** are conserved but differences exist in the rim region of the binding

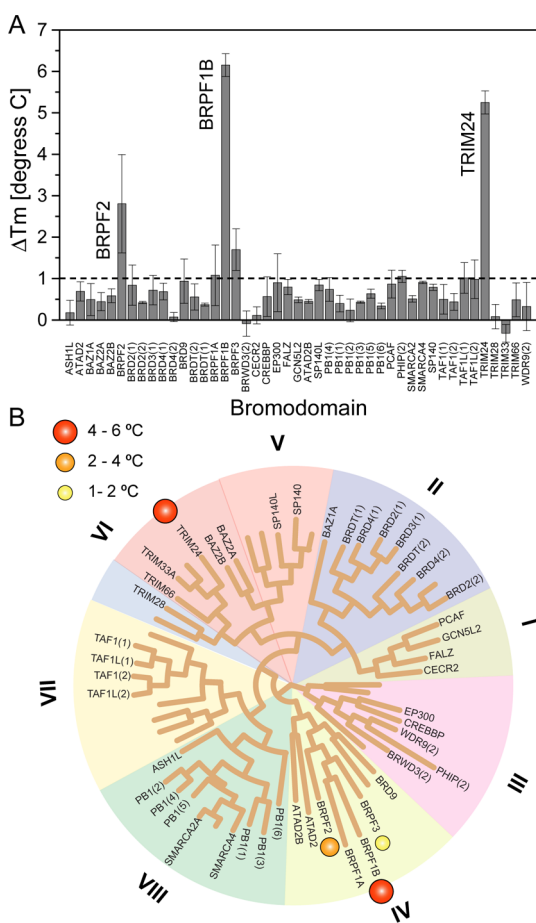


**Figure 2.** Selectivity of **34**. (A) Shown are temperature shift data ( $\Delta T_m$ ) for 45 human bromodomains. The bar diagram shows the mean of three replicates as well as the standard error.  $\Delta T_m$  smaller than 1 degree were not considered significant as indicated by a dotted line. (B) Temperature shifts mapped to the phylogenetic tree of the human bromodomain family.  $\Delta T_m$  are represented as circles as indicated in the figure.

sites that may be used for the design of selective TRIM24 inhibitors.

Cellular activity of **34** was demonstrated using FRAP (fluorescent recovery after photobleaching) assays<sup>33</sup> (Figure 4).

FRAP experiments showed that **34** effectively reduced fluorescent recovery half-time at 1  $\mu\text{M}$  concentration for full length TRIM24 fused to GFP to levels similar to the bromodomain inactivating mutant N980F, suggesting that the inhibitor effectively displaces TRIM24 from chromatin. Full length BRPF1B linked to GFP showed, however, predominantly cytoplasmic expression, prohibiting development of FRAP assays. To demonstrate that the bromodomain of BRPF1B is inhibited in the nucleus of cells, we used a construct containing a triplicated bromodomain and a nuclear localization signal. To increase affinity of this construct further, we also increased global acetylation levels using the pan-HDAC inhibitor SAHA. BRPF bromodomains have been shown to interact with H4K12ac and H2AK5ac with modest affinity (50–80  $\mu\text{M}$ ), explaining the small assay window and the small increase of recovery times after exposure to SAHA.<sup>34</sup> However, the strategy adding SAHA provided a sufficiently large assay window for the triplicated BRPF1B construct as reported for the bromodomain in CBP.<sup>9,33</sup> For this construct, the bromodomain inactivating mutant showed significantly reduced

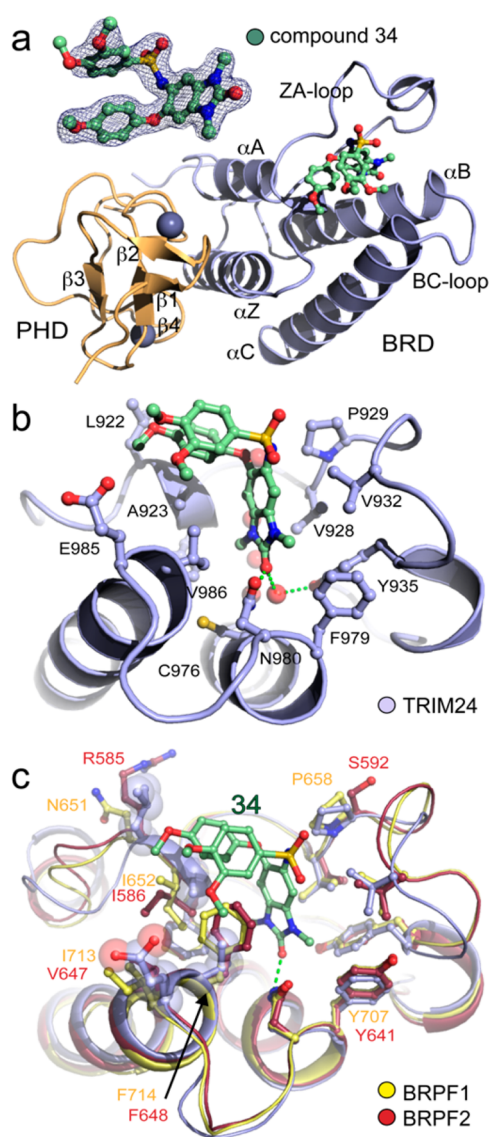


**Figure 3.** Structure of the TRIM24 complex with **34**. (a)  $2F_o - F_c$  density map contoured at  $2\sigma$  around **34** and ribbon diagram of the PHD and bromodomain structure. The main structural elements are labeled. The inhibitor is shown in ball and stick representation.  $\text{Zn}^{2+}$  atoms are shown as spheres. (b) Details of the interaction of **34** with the TRIM24 acetyl-lysine binding site. (c) Comparison of the acetyl-lysine binding site of the bromodomains of BRPF1B and BRD1 (BRPF2). Carbon atoms of residues present in each structure are colored as indicated in the figure. Further comparisons of structural features of BRPF and TRIM24 bromodomains as well as a sequence alignment have been included in Supporting Information Figure 2.

recovery time. The inhibitor **34** also reduced recovery times, supporting target engagement of the compound.

Because overexpression of TRIM24 has been linked to tumorigenesis, we tested the effect of compound **34** on a small panel of diverse cancer cell lines. However, **34** showed no significant cytotoxicity in the cell lines tested (Figure 5). The breast cancer cell line MCF-7 was resistant to TRIM24 bromodomain inhibition in the concentration range tested, whereas other cell lines such as the myeloma MM1S model showed modest sensitivity ( $\text{GI}_{50} > 10 \mu\text{M}$ ). A more comprehensive evaluation of the role of TRIM24 in cancer cell proliferation and chromatin biology would require the development of a tool compound with improved selectivity.



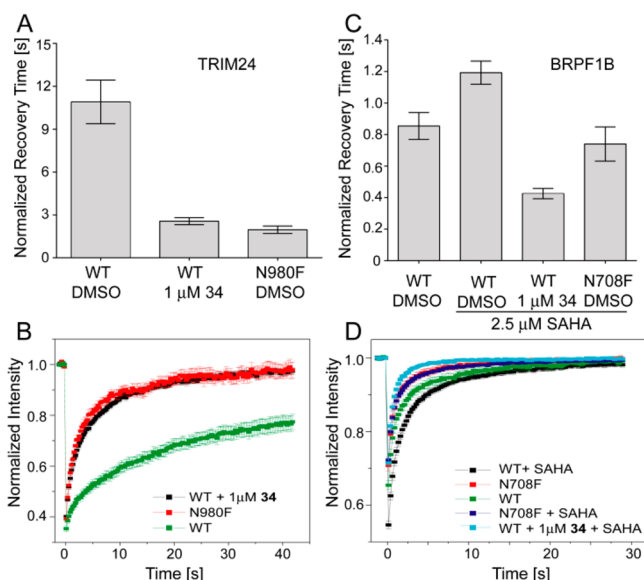


**Figure 4.** FRAP assays. (A) Fluorescent recovery half-lives for TRIM24. (B) Time dependence of the fluorescent recovery of the bleached area. (C) Fluorescent recovery half-lives for the BRPF1B bromodomain construct. (D) Time dependence of the fluorescent recovery of the bleached area for BRPF1B. At least 10 nuclei were bleached for each experiment, and the mean recovery time as well as the SEM are shown in (A) and (C).

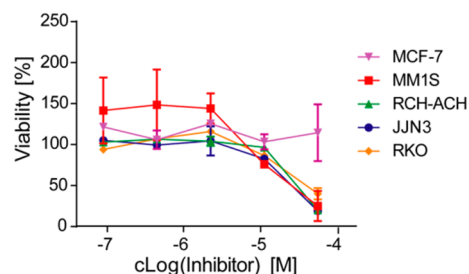


**Figure 5.** Cell viability affected by 34 for a selection of cancer cell lines.

## CONCLUSION

In this study we identified a potent TRIM24/BRPF1/2 dual inhibitor (34) that was selective for these bromodomains when screened against a comprehensive panel of bromodomains. However, selectivity of this inhibitor series between TRIM24 and BRPF bromodomains was not achieved with this series. The cocrystal structure in complex with the bromo/PHD domain of TRIM24 revealed an acetyl-lysine mimetic binding mode of the benzimidazolone moiety and a stacked conformation of the two aromatic decorations, creating a good shape complementarity with the TRIM24 binding site. The identified inhibitor was cell active and displaced ectopically expressed full-length TRIM24 from chromatin. The identified TRIM24 inhibitor had modest cytotoxicity on a panel of cancer cell lines. The presented SAR and the identified inhibitor represents an excellent starting point for further optimization of TRIM24 inhibitors as well as a valuable tool for better understanding of the biology of the targeted bromodomain proteins.

## ASSOCIATED CONTENT

### Supporting Information

Experimental details, crystallographic data, and additional screening data. The Supporting Information is available free of charge on the ACS Publications website at DOI: 10.1021/acs.jmedchem.5b00458.

## AUTHOR INFORMATION

### Corresponding Author

\*Phone: +49 69 79 82 98 71. E-mail: Knapp@pharmchem.uni-frankfurt.de.

### Notes

The authors declare the following competing financial interest(s): B. Haendler is a full-time employee of Bayer Pharma AG.

## ACKNOWLEDGMENTS

The SGC is a registered charity (no. 1097737) that receives funds from AbbVie, Bayer Pharma AG, Boehringer Ingelheim, the Canada Foundation for Innovation, Genome Canada, GlaxoSmithKline, Janssen, Lilly Canada, the Novartis Research Foundation, the Ontario Ministry of Economic Development and Innovation, Pfizer, Takeda, and the Wellcome Trust [092809/Z/10/Z]. We would like to thank Chandra Ramarao (Avra Laboratories) for the gift of compound 7. J. Meier is supported by a postdoctoral grant from Bayer Pharma AG.

## REFERENCES

- Muller, S.; Filippakopoulos, P.; Knapp, S. Bromodomains as therapeutic targets. *Expert Rev. Mol. Med.* **2011**, *13*, e29.
- Filippakopoulos, P.; Knapp, S. Targeting bromodomains: epigenetic readers of lysine acetylation. *Nature Rev. Drug Discovery* **2014**, *13*, 337–356.
- Filippakopoulos, P.; Qi, J.; Picaud, S.; Shen, Y.; Smith, W. B.; Fedorov, O.; Morse, E. M.; Keates, T.; Hickman, T. T.; Felletar, I.; Philpott, M.; Munro, S.; McKeown, M. R.; Wang, Y.; Christie, A. L.; West, N.; Cameron, M. J.; Schwartz, B.; Heightman, T. D.; La Thangue, N.; French, C. A.; Wiest, O.; Kung, A. L.; Knapp, S.; Bradner, J. E. Selective inhibition of BET bromodomains. *Nature* **2010**, *468*, 1067–1073.
- Dawson, M. A.; Prinjha, R. K.; Dittmann, A.; Giotopoulos, G.; Bantscheff, M.; Chan, W. I.; Robson, S. C.; Chung, C. W.; Hopf, C.; Savitski, M. M.; Huthmacher, C.; Gudgin, E.; Lugo, D.; Beinke, S.; Chapman, T. D.; Roberts, E. J.; Soden, P. E.; Auger, K. R.; Mirguet, O.; Doehner, K.; Delwel, R.; Burnett, A. K.; Jeffrey, P.; Drewes, G.; Lee, K.; Huntly, B. J.; Kouzarides, T. Inhibition of BET recruitment to chromatin as an effective treatment for MLL-fusion leukaemia. *Nature* **2011**, *478*, 529–533.
- Delmore, J. E.; Issa, G. C.; Lemieux, M. E.; Rahl, P. B.; Shi, J.; Jacobs, H. M.; Kastiris, E.; Gilpatrick, T.; Paranal, R. M.; Qi, J.; Chesi, M.; Schinzel, A. C.; McKeown, M. R.; Heffernan, T. P.; Vakoc, C. R.; Bergsagel, P. L.; Ghobrial, I. M.; Richardson, P. G.; Young, R. A.; Hahn, W. C.; Anderson, K. C.; Kung, A. L.; Bradner, J. E.; Mitsiades, C. S. BET bromodomain inhibition as a therapeutic strategy to target c-Myc. *Cell* **2011**, *146*, 904–917.
- Picaud, S.; Da Costa, D.; Thanasopoulou, A.; Filippakopoulos, P.; Fish, P. V.; Philpott, M.; Fedorov, O.; Brennan, P.; Bunnage, M. E.; Owen, D. R.; Bradner, J. E.; Taniere, P.; O'Sullivan, B.; Muller, S.; Schwaller, J.; Stankovic, T.; Knapp, S. PFI-1, a highly selective protein interaction inhibitor, targeting BET Bromodomains. *Cancer Res.* **2013**, *73*, 3336–3346.
- Cheng, Z.; Gong, Y.; Ma, Y.; Lu, K.; Lu, X.; Pierce, L. A.; Thompson, R. C.; Muller, S.; Knapp, S.; Wang, J. Inhibition of BET bromodomain targets genetically diverse glioblastoma. *Clin. Cancer Res.* **2013**, *19*, 1748–1759.

- (8) Nicodeme, E.; Jeffrey, K. L.; Schaefer, U.; Beinke, S.; Dewell, S.; Chung, C. W.; Chandwani, R.; Marazzi, I.; Wilson, P.; Coste, H.; White, J.; Kirilovsky, J.; Rice, C. M.; Lora, J. M.; Prinjha, R. K.; Lee, K.; Tarakhovskiy, A. Suppression of inflammation by a synthetic histone mimic. *Nature* **2010**, *468*, 1119–1123.
- (9) Hay, D. A.; Fedorov, O.; Martin, S.; Singleton, D. C.; Tallant, C.; Wells, C.; Picaud, S.; Philpott, M.; Monteiro, O. P.; Rogers, C. M.; Conway, S. J.; Rooney, T. P.; Tumber, A.; Yapp, C.; Filippakopoulos, P.; Bunnage, M. E.; Muller, S.; Knapp, S.; Schofield, C. J.; Brennan, P. E. Discovery and optimization of small-molecule ligands for the CBP/p300 bromodomains. *J. Am. Chem. Soc.* **2014**, *136*, 9308–9319.
- (10) Fedorov, O.; Lingard, H.; Wells, C.; Monteiro, O. P.; Picaud, S.; Keates, T.; Yapp, C.; Philpott, M.; Martin, S. J.; Felletar, I.; Marsden, B. D.; Filippakopoulos, P.; Muller, S.; Knapp, S.; Brennan, P. E. [1,2,4]Triazololo[4,3-*a*]phthalazines: inhibitors of diverse bromodomains. *J. Med. Chem.* **2014**, *57*, 462–476.
- (11) Demont, E. H.; Bamborough, P.; Chung, C. W.; Craggs, P. D.; Fallon, D.; Gordon, L. J.; Grandi, P.; Hobbs, C. I.; Hussain, J.; Jones, E. J.; Le Gall, A.; Michon, A. M.; Mitchell, D. J.; Prinjha, R. K.; Roberts, A. D.; Sheppard, R. J.; Watson, R. J. 1,3-Dimethyl Benzimidazolones Are Potent, Selective Inhibitors of the BRPF1 Bromodomain. *ACS Med. Chem. Lett.* **2014**, *5*, 1190–1195.
- (12) Rooney, T. P.; Filippakopoulos, P.; Fedorov, O.; Picaud, S.; Cortopassi, W. A.; Hay, D. A.; Martin, S.; Tumber, A.; Rogers, C. M.; Philpott, M.; Wang, M.; Thompson, A. L.; Heightman, T. D.; Pryde, D. C.; Cook, A.; Paton, R. S.; Muller, S.; Knapp, S.; Brennan, P. E.; Conway, S. J. A series of potent CREBBP bromodomain ligands reveals an induced-fit pocket stabilized by a cation– $\pi$  interaction. *Angew. Chem., Int. Ed. Engl.* **2014**, *53*, 6126–6130.
- (13) Vidler, L. R.; Brown, N.; Knapp, S.; Hoelder, S. Druggability analysis and structural classification of bromodomain acetyl-lysine binding sites. *J. Med. Chem.* **2012**, *55*, 7346–7359.
- (14) Filippakopoulos, P.; Picaud, S.; Mangos, M.; Keates, T.; Lambert, J. P.; Barsyte-Lovejoy, D.; Felletar, I.; Volkmer, R.; Muller, S.; Pawson, T.; Gingras, A. C.; Arrowsmith, C. H.; Knapp, S. Histone recognition and large-scale structural analysis of the human bromodomain family. *Cell* **2012**, *149*, 214–231.
- (15) Filippakopoulos, P.; Knapp, S. The bromodomain interaction module. *FEBS Lett.* **2012**, *586*, 2692–2704.
- (16) Vidler, L. R.; Filippakopoulos, P.; Fedorov, O.; Picaud, S.; Martin, S.; Tomsett, M.; Woodward, H.; Brown, N.; Knapp, S.; Hoelder, S. Discovery of novel small-molecule inhibitors of BRD4 using structure-based virtual screening. *J. Med. Chem.* **2013**, *56*, 8073–8088.
- (17) Ciceri, P.; Muller, S.; O'Mahony, A.; Fedorov, O.; Filippakopoulos, P.; Hunt, J. P.; Lasater, E. A.; Pallares, G.; Picaud, S.; Wells, C.; Martin, S.; Wodicka, L. M.; Shah, N. P.; Treiber, D. K.; Knapp, S. Dual kinase–bromodomain inhibitors for rationally designed polypharmacology. *Nature Chem. Biol.* **2014**, *10*, 305–312.
- (18) Ember, S. W.; Zhu, J. Y.; Olesen, S. H.; Martin, M. P.; Becker, A.; Berndt, N.; Georg, G. I.; Schonbrunn, E. Acetyl-lysine binding site of bromodomain-containing protein 4 (BRD4) interacts with diverse kinase inhibitors. *ACS Chem. Biol.* **2014**, *9*, 1160–1171.
- (19) Tsai, W. W.; Wang, Z.; Yiu, T. T.; Akdemir, K. C.; Xia, W.; Winter, S.; Tsai, C. Y.; Shi, X.; Schwarzer, D.; Plunkett, W.; Aronow, B.; Gozani, O.; Fischle, W.; Hung, M. C.; Patel, D. J.; Barton, M. C. TRIM24 links a non-canonical histone signature to breast cancer. *Nature* **2010**, *468*, 927–932.
- (20) Zhang, L. H.; Yin, A. A.; Cheng, J. X.; Huang, H. Y.; Li, X. M.; Zhang, Y. Q.; Han, N.; Zhang, X. TRIM24 promotes glioma progression and enhances chemoresistance through activation of the PI3K/Akt signaling pathway. *Oncogene* **2015**, *34*, 600–610.
- (21) Liu, X.; Huang, Y.; Yang, D.; Li, X.; Liang, J.; Lin, L.; Zhang, M.; Zhong, K.; Liang, B.; Li, J. Overexpression of TRIM24 is associated with the onset and progress of human hepatocellular carcinoma. *PLoS One* **2014**, *9*, e85462.
- (22) Miao, Z. F.; Wang, Z. N.; Zhao, T. T.; Xu, Y. Y.; Wu, J. H.; Liu, X. Y.; Xu, H.; You, Y.; Xu, H. M. TRIM24 is upregulated in human gastric cancer and promotes gastric cancer cell growth and chemoresistance. *Virchows Arch.* **2015**, *466*, 525–532.
- (23) Li, H.; Sun, L.; Tang, Z.; Fu, L.; Xu, Y.; Li, Z.; Luo, W.; Qiu, X.; Wang, E. Overexpression of TRIM24 correlates with tumor progression in non-small cell lung cancer. *PLoS One* **2012**, *7*, e37657.
- (24) Cui, Z.; Cao, W.; Li, J.; Song, X.; Mao, L.; Chen, W. TRIM24 overexpression is common in locally advanced head and neck squamous cell carcinoma and correlates with aggressive malignant phenotypes. *PLoS One* **2013**, *8*, e63887.
- (25) Theurillat, J. P.; Udeshi, N. D.; Errington, W. J.; Svinkina, T.; Baca, S. C.; Pop, M.; Wild, P. J.; Blattner, M.; Groner, A. C.; Rubin, M. A.; Moch, H.; Prive, G. G.; Carr, S. A.; Garraway, L. A. Prostate cancer. Ubiquitylome analysis identifies dysregulation of effector substrates in SPOP-mutant prostate cancer. *Science* **2014**, *346*, 85–89.
- (26) Allton, K.; Jain, A. K.; Herz, H. M.; Tsai, W. W.; Jung, S. Y.; Qin, J.; Bergmann, A.; Johnson, R. L.; Barton, M. C. Trim24 targets endogenous p53 for degradation. *Proc. Natl. Acad. Sci. U. S. A.* **2009**, *106*, 11612–11616.
- (27) Le Douarin, B.; Nielsen, A. L.; Garnier, J. M.; Ichinose, H.; Jeanmougin, F.; Losson, R.; Chambon, P. A possible involvement of TIF1 alpha and TIF1 beta in the epigenetic control of transcription by nuclear receptors. *EMBO J.* **1996**, *15*, 6701–6715.
- (28) Wang, J.; Zhu, J.; Dong, M.; Yu, H.; Dai, X.; Li, K. Knockdown of tripartite motif containing 24 by lentivirus suppresses cell growth and induces apoptosis in human colorectal cancer cells. *Oncol. Res.* **2014**, *22*, 39–45.
- (29) Pathiraja, T. N.; Thakkar, K. N.; Jiang, S.; Stratton, S.; Liu, Z.; Gagea, M.; Shi, X.; Shah, P. K.; Phan, L.; Lee, M. H.; Andersen, J.; Stampfer, M.; Barton, M. C. TRIM24 links glucose metabolism with transformation of human mammary epithelial cells. *Oncogene* **2014**, DOI: 10.1038/onc.2014.220.
- (30) Khetchoumian, K.; Teletin, M.; Tisserand, J.; Mark, M.; Herquel, B.; Ignat, M.; Zucman-Rossi, J.; Cammas, F.; Lerouge, T.; Thibault, C.; Metzger, D.; Chambon, P.; Losson, R. Loss of Trim24 (Tif1alpha) gene function confers oncogenic activity to retinoic acid receptor alpha. *Nature Genet.* **2007**, *39*, 1500–1506.
- (31) Fedorov, O.; Niesen, F. H.; Knapp, S. Kinase inhibitor selectivity profiling using differential scanning fluorimetry. *Methods Mol. Biol.* **2012**, *795*, 109–118.
- (32) Drouin, L.; McGrath, S.; Vidler, L. R.; Chaikuad, A.; Monteiro, O.; Tallant, C.; Philpott, M.; Rogers, C.; Fedorov, O.; Liu, M.; Akhtar, W.; Hayes, A.; Raynaud, F.; Muller, S.; Knapp, S.; Hoelder, S. Structure Enabled Design of BAZ2-ICR, A Chemical Probe Targeting the Bromodomains of BAZ2A and BAZ2B. *J. Med. Chem.* **2015**, *58*, 2553–2559.
- (33) Philpott, M.; Rogers, C. M.; Yapp, C.; Wells, C.; Lambert, J. P.; Strain-Damerell, C.; Burgess-Brown, N. A.; Gingras, A. C.; Knapp, S.; Muller, S. Assessing cellular efficacy of bromodomain inhibitors using fluorescence recovery after photobleaching. *Epigenetics Chromatin* **2014**, *7*, 14.
- (34) Poplawski, A.; Hu, K.; Lee, W.; Natesan, S.; Peng, D.; Carlson, S.; Shi, X.; Balaz, S.; Markley, J. L.; Glass, K. C. Molecular insights into the recognition of N-terminal histone modifications by the BRPF1 bromodomain. *J. Mol. Biol.* **2014**, *426*, 1661–1676.